Seismic Probabilistic Risk Assessment of Structures and Internal Equipment in Retaining Wall Collisions of Seismically Isolated Reactor Buildings

Takeshi Nomura[1], Yasuki Ohtori[1], Hitoshi Muta[1], Yoshihumi Katayama[2]

[1]1Tokyo City University, 1-28-1 Tamazutsumi, Setagaya-ku, Tokyo 158-8557, Japan
[2] Chuden Engineering Consultants, Hiroshima, Japan

ABSTRACT

Seismically isolated structures reduce seismic forces by shifting the natural period to longer periods and dissipating input energy. When ground motions exceed the design level, collisions between the structure and surrounding retaining walls could occur. These collisions can generate impact forces that exceed the design capacities of both the structure and internal equipment. Although previous studies have mainly focused on structural responses to such collisions, the risk of internal equipment damage, which could trigger severe accidents in nuclear facilities, remains unevaluated. This study conducts a probabilistic risk assessment of internal equipment damage caused by retaining wall collisions in seismically isolated nuclear reactor buildings. We generated 30 structural models using Latin Hypercube Sampling, considering aleatory uncertainty in models. Nonlinear time history analyses were performed using input ground motions with peak ground accelerations from 1 to 40 m/s^2. We calculated floor response accelerations at natural periods of 0.1, 0.5, and 1.0 s, and developed fragility curves incorporating epistemic uncertainty caused by the collisions. The results indicate that retaining wall collisions can damage internal equipment before structural failure. Upon collision, impact-force uncertainty rises, leading to greater variability in floor response accelerations on equipment. At high design capacity levels, this collision-induced uncertainty expands response variability and increases β in the fragility curve. Our findings emphasize the need to evaluate not only structural response but also internal equipment vulnerability to ensure the seismic safety of nuclear facilities.

Keywords: Seismic Response Analysis, Seismically Isolated Structures, Seismic PRA

I. INTRODUCTION

Seismically isolated structures reduce external seismic forces significantly by shifting the natural period to longer periods and dissipating input seismic energy. When ground motions exceed the design level, seismically isolated structures may not fully absorb seismic energy. In such cases, the impact force caused by collisions with the surrounding retaining wall may exceed the design capacity of both the structure and the internal equipment.

Although previous studies have evaluated structural responses, no risk assessment has specifically addressed damage to internal equipment, whose failure could directly lead to severe accidents in seismically isolated nuclear facilities [1]-[5]. NAKANISHI et al. examined wall-collision effects on a seismically isolated structure, reporting on first-story inter-story drift angles and the probability of structural damage under seismic loading [6]. NAKAZAWA et al. investigated how wall impacts influence the yielding ratio of the superstructure [7]. SAREBANHA et al. studied their effects on maximum bearing displacement and residual deformation in the isolation layer [8]. All these prior studies limited their damage evaluations to the superstructure and laminated rubber bearings, leaving the vulnerability of internal equipment unaddressed. The studies that do not consider internal equipment risk failing to accurately evaluate severe accidents.

Based on these studies, we compared the effects on structure and internal equipment of retaining wall collisions in seismically isolated nuclear power buildings. We considered both aleatory uncertainty (βa; structure material uncertainty) and epistemic uncertainty (βe; collision uncertainty) to evaluate the seismic risk to internal equipment [9]. We conducted nonlinear seismic response analyses using the dynamic-analysis software TDAP3[10]. The results indicate three key points.

(1) Previous studies mainly focused on superstructures and isolation layers. However, retaining wall collisions can also damage internal equipment. Such damage in nuclear facilities can lead to severe accidents or serious consequences.
(2) Upon collision, the uncertainty associated with impact forces increases, consequently increasing the variability of floor response accelerations acting on internal equipment.
(3) When design capacity is high, the increased uncertainty due to collisions results in greater variability of responses, thus increasing the uncertainty parameter β of the fragility curve.

This paper is composed as follows: II. Analysis Model, Ⅲ.Analysis Outline, Ⅳ.Results, and Ⅴ.Conclusions.

II. ANALYSIS MODEL

In this study, the analysis model was a 2D single-axis, multi-degree-of-freedom mass model. Fig.1 shows the overall of the model. This model reflected the mass ratios characteristics of nuclear power building based on prior research [11]. Miwata et al. found minor difference between 2D and 3D models for the wall-collision phenomenon in seismically isolated structures, although researchers sometimes use 3D models to examine this case [12]. Table.1 shows the material properties and other factors of the model.

Table I. Model Parameters List

Total mass(ton)	178948	Structure 1st period (s)	8.9743E-1
Isolation period (s)	3.00	Structure 2nd period (s)	3.9231E-1
Rayleigh damping 1st frequency (Hz)	1.06	Structure3rd period (s)	3.1576E-1
Rayleigh damping 2nd frequency (Hz)	51.1	Structure 4th period (s)	1.0926E-1

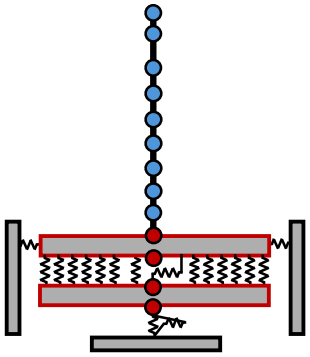

FIGURE 1. Analysis Model

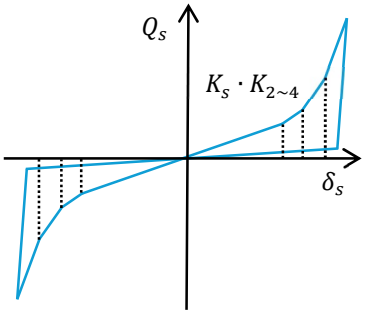

FIGURE 2. Laminated-Rubber Stiffness Model

II. A. Superstructure

The superstructure is a single-axis nine–degree-of-freedom mass model assuming a prestressed concrete containment vessel of the material. Each mass element incorporates nonlinear behavior. The shear direction restoring force behavior is represented by a peak oriented trilinear model, while the bending restoring force behavior is represented by a trilinear mode. We did not consider the mass of internal equipment because it was negligible relative to the total structural mass.

II. B. Seismic Isolation Layer

We set the seismic isolation period as 3 s because it is generally in the 2-4 s range. The isolation layer comprises a laminated-rubber stiffness model with hardening considered as Fig. 2, a lead plug stiffness model as Fig. 3 and collision wall stiffness model as Fig. 4. Laminated-rubber stiffness model and lead plug stiffness model were with the devices installed beneath the superstructure. The isolation layer comprises an upper foundation slab, a lower foundation slab, horizontal ground springs, vertical and rotational ground springs at the soil interface, and vertical and horizontal isolation springs. We designated the central node as the primary degree and the other nodes as dependent points.

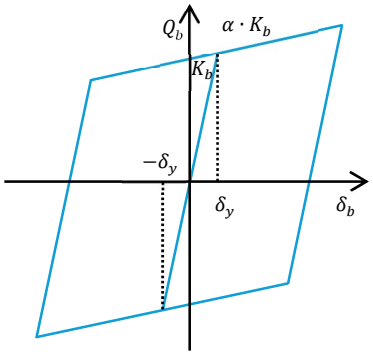

FIGURE 3. Lead Plug Stiffness Model

II.B.1. Laminated Rubber Stiffness Model

Fig. 2 shows the laminated rubber shear spring model. Its initial stiffness is 7.85×10^5 N/m, with post-hardening stiffness increase ratios of 1.5, 2.0, and 4.0. The laminated-rubber element was assumed to have a linear-limit shear strain of 250 % (0.55 m) and a failure limit of 450 % (0.99 m) based on prior research [13]. We set a 0.6 m clearance between the edges of the isolation layer and the retaining wall. A single horizontal isolation spring was consolidated at the midpoint between the upper and lower foundation slabs.

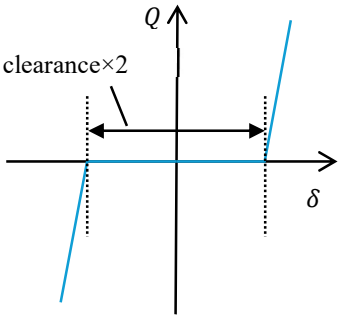

FIGURE 4. Collision wall Stiffness Model

II.B.2. Lead Plug Stiffness Model

Fig. 3 shows the bilinear model for the lead plug. Its initial stiffness is 7.06×10^6 N/m, and the yield displacement $\boldsymbol{\delta_b}$ defined by dividing the yield load by the equivalent stiffness—was set to 0.0124 m. Although the post-yield stiffness was idealized as zero, a small nonzero value was assigned to prevent numerical errors. Both nonlinear models exhibit slip behavior in accordance with Masing's hysteresis rule.

II.B.3. Collision Wall Stiffness Model

Fig.4 shows the collision wall stiffness model. The linear stiffness we defined was as a value near zero. The nonlinear stiffness based on prior research was increasing rapidly upon contact thereby retaining wall collision. T_w=0.05 s as the rigid structure's natural period and M = 178948 t as the total mass equals K_w= 2.826×10^9 kN/cm [14].

II. C. Latin Hypercube Sampling

We performed sensitivity analyses using II. ANALYSIS MODEL on parameters known from previous studies to influence wall pounding, varying each parameter by ±10% in 1% increments (21 cases). From those results, we compared the maximum first-floor acceleration at a natural period of 0.1 s. For the six parameters that exhibited no clear response trends, we assigned coefficients of variation (COV) based on research and generated 30 models via Latin Hypercube Sampling (LHS) over a log-normal distribution, Table 2. Kikuchi et al. performed risk assessment without COV whereas we introduced one to consider uncertainty in our analysis [15]. Hayashi et al. showed that the superstructure's COV depends on its damage state [16]. Retaining wall collisions occur before the superstructure sustains damage, except when wall stiffness is extremely low. We assumed a minor damage state for the superstructure for the safety side. [6] Because the surrounding retaining wall natural period of this model is 0.05s as the rigid structure.

Table II. LHS Parameters List

	Lead plug 1st stiffness [17] (N/m)	Lead damper yield point [18]	Laminated rubber 1st stiffness [18] (N/m)	Superstructure 1st stiffness [16] (N/m)	Superstructure shear strain [9]	Collision wall stiffness [19] (N/m)
Median	7.060×10^6	0.0124	7.850×10^5	2.050×10^5	2.120×10^{-4}	2.826×10^9
COV	0.05	0.05	0.05	0.08	0.253	0.10

III. ANALYSIS OUTLINE

III. A. Input ground motion

We generated the horizontal input ground-motion time history using Katayama's method, which is based on the amplitude-envelope function of Noda et al. (2002) to match the uniform hazard spectrum [20]. We then set the vertical component to two-thirds of the horizontal component. Fig. 5 shows the input time history acceleration. Fig. 6 shows the uniform hazard spectrum.

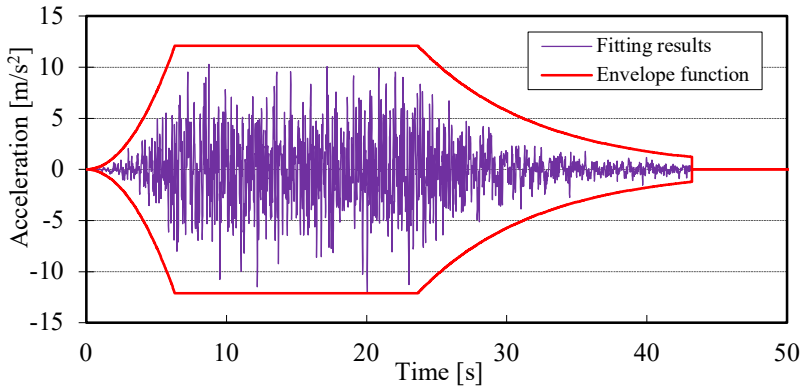

FIGURE 5. Input Time History Acceleration

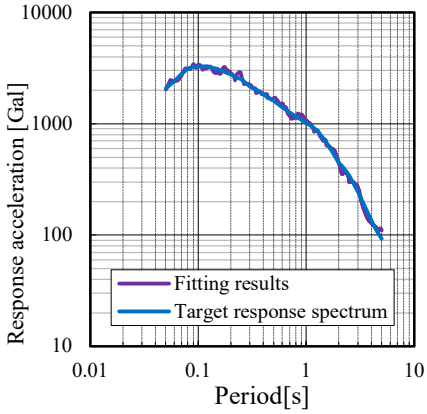

FIGURE 6. Unform Hazard Spectrum

III. B. Seismic risk assessment method

III. B.1 Nonlinear analysis and floor response

We conducted nonlinear analysis combining 30 models created by LHS (II. D) and ground motion with peak ground acceleration (PGA) of 1 to 40 m/s^2 (III. A). Based on prior research, we set the integration time step to 0.00001 s based on prior research where results were stable. Collisions occurred in every model up to 40 m/s^2. We compared structural inter-story drift angles with the floor response accelerations experienced by internal equipment at natural periods of 0.1, 0.5, and 1.0 s. We calculated the median floor response spectrum of 30 models under PGA of 1 to 40 m/s^2.

III. B.2 fragility curve

We assigned a log-normal probability density function to the plotted floor response acceleration in *III. B.1* as median value. We set σ to 0.3 and 0.6 for the collision cases, considering β_e caused by the collision phenomenon [21], and σ to 0.1 for the no collision case. We obtained the probability of exceedance: P_i by comparing a log-normal distribution with the 150, 300, 450 m/s^2 set as the design capacity (DC) of the internal equipment [22]. We calculated damage probability: P_n at each 1 m/s^2 increment of PGA and plotted fragility curves from PGA of 1 to 40 m/s^2.

IV. RESULT

Figure 7 shows a comparison of damage to internal equipment and structures. The X-axis shows the impact on internal equipment by plotting the median first floor response acceleration among 30 models at each PGA, and the Y-axis shows the impact on the building, by plotting the median inter-story drift angles among 30 models at each PGA. We assumed natural periods of 0.1, 0.5, and 1.0 s. We set the DC of internal equipment to 77.8 m/s² for electrical panel functionality (black dotted line) [22] and the DC of structure to an inter-story drift angle of 1/60 (black solid line) [6]. We assumed internal equipment natural periods of 0.1 (red), 0.5 (green), and 1.0 s (pink). For the longer periods (0.5 s, 1.0 s), the inter-story drift angle reached 1/60 at a PGA of 26 m/s² before the internal equipment DC was exceeded, indicating that the structure sustains damage first. In contrast, at a natural period of 0.1 s, both internal equipment and the structure exceed their DC at the same PGA of 26 m/s. Previous studies of seismically isolated structures with retaining walls collisions have focused mainly on structural damage. However internal equipment failure can cause total loss of function and serve accidents. Therefore, we should also evaluate damage to internal equipment.

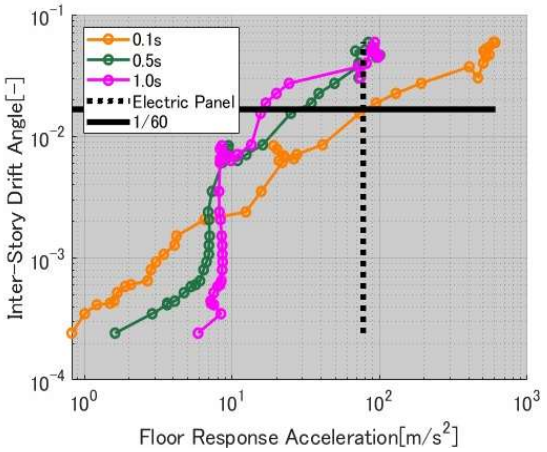

Figure 7. Comparison of structures and internal equipment

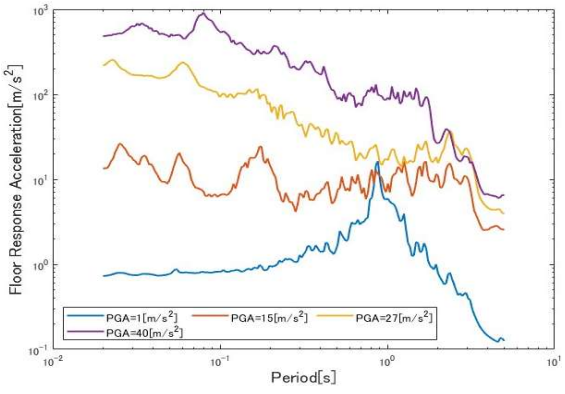

Figure 8. Floor Response Acceleration Spectrum

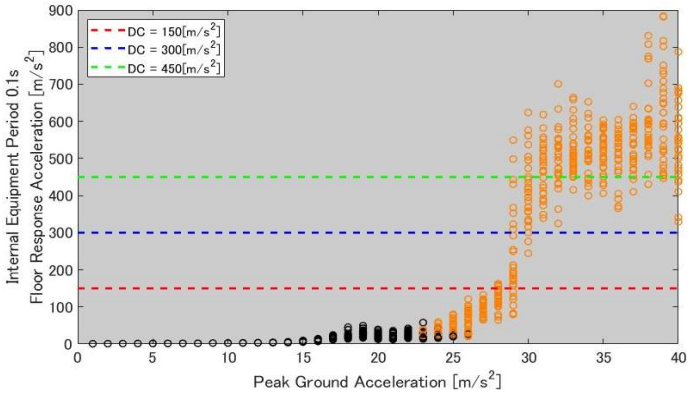

Figure 9. Peak Ground acceleration with natural period of 0.1s for 1200 cases

Fig.8 shows the floor response acceleration spectrum in case of PGA 1,15,27,40 m/s^2 as described in section *III. B.1*. Retaining wall collisions increase the response spectrum on the short-period side. This is from retaining wall collision and hardening effect of the laminated rubber layer caused by excessive seismic motion.

Fig.9 shows the first-floor response accelerations at natural period of 0.1s for 30 models under PGA of 1 to 40 m/s^2 from Fig.8. We change the collided case color from black to orange. The collision begins when the PGA reached 23 m/s^2 in several models. The variation of floor response acceleration after the collision is larger than before the collision caused the uncertainty collision phenomenon yield. We consider this factor responsible for the difference between those that exceed the DC and those that do not, Among the 30 models which occurred collision.

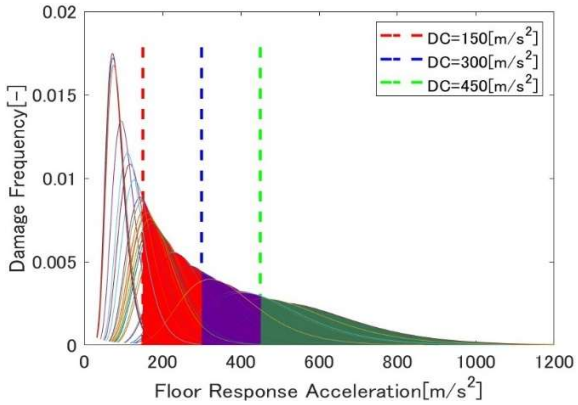

Figure 10. In β_e = 0.3, Variation of floor response acceleration at PGA 29m/s²

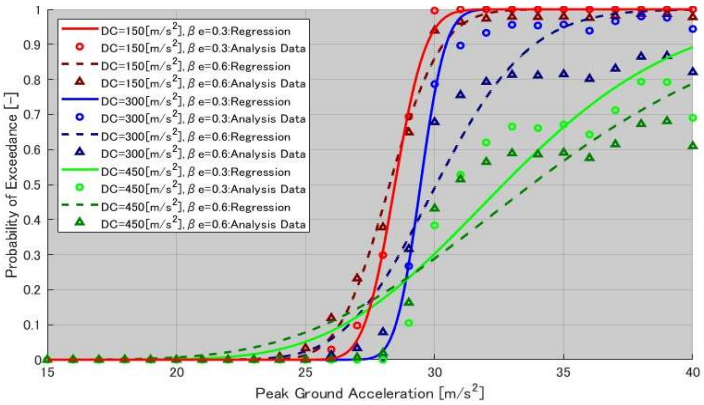

Figure 11. Fragility Curve

Table III. Regression Fragility Curve Am and β List

	DC=150, β_e=0.3	DC=150, β_e=0.6	DC=300, β_e=0.3	DC=300, β_e=0.6	DC=450, β_e=0.3	DC=450, β_e=0.6
Am	28.5	28.3	29.4	30.1	32.7	33.8
β	0.033	0.055	0.026	0.093	0.163	0.212

Fig.10 shows the probability density function given a log-normal distribution for the 30 points plotted for one PGA in Fig.9. We calculated the probability of damage: P_n by comparing log-normal distribution with DC.

Fig. 11 plots the damage probabilities for PGA values from 1 to 40 m/s², as calculated in Fig. 10. We rescaled the x axis to display PGA from 15 to 40 m/s². The solid line plots the regression fragility curve obtained by nonlinear optimization with β_e=0.3, the dashed line plots the regression fragility curve obtained by nonlinear optimization with β_e=0.6, and the markers plot the analysis data. Table.3 shows that β increases for β_e = 0.6 compared to β_e = 0.3 for all DC, indicating that the regression fragility curve for β_e = 0.6 rises more slowly than that for β_e = 0.3. This occurs because using β_e = 0.6 as the log-normal standard deviation in Fig. 10 yields a distribution wider than β_e = 0.3. From figures 9 and 11, we considered when DC is low, the floor response exceeds DC before variability in response arises, resulting in a small fragility-curve β. Therefore, for DC = 150 m/s², the damage probability increases sharply. While when DC is high, collision uncertainty increases response variability, which raises the fragility-curve β. For DC = 300 and 450 m/s², beyond a PGA of 35 m/s² —where significant large collisions occur— the gap between models that exceed DC and those that do not widen, resulting in damage probability increasing gradually than DC = 150 m/s².

V. CONCLUSIONS

In this study, we performed a risk assessment of damage to internal equipment caused by retaining wall collisions in seismically isolated nuclear reactor buildings. To consider aleatory uncertainty in structural model parameters, we generated 30 structural models using Latin Hypercube Sampling. We generated uniform hazard spectra using an amplitude envelope function and conducted nonlinear time history analyses with input ground motions having peak ground accelerations of 1 to 40 m/s². From the analysis results, we compared the responses of internal equipment and the superstructure. To evaluate the failure probability of internal equipment, we developed fragility curves considering the epistemic uncertainty associated with collision. The following 3 points are clarified in this study:

(1) Previous studies mainly focused on superstructures and isolation layers. However, retaining wall collisions can also damage internal equipment. Such damage to nuclear facilities can lead to severe accidents or serious consequences.
(2) Upon collision, the uncertainty associated with impact forces increases, consequently increasing the variability of floor response accelerations acting on internal equipment.
(3) When DC is high, the increased uncertainty due to collisions results in greater variability of responses, thus increasing the uncertainty parameter β of the fragility curve.

Attention should be paid to the design capacity and clearance between the retaining wall and the isolation layer. In future research, we will design and evaluate seismically isolated structures to optimize the balance between risk and cost.

REFERENCES

[1] Y.MARA,Y.AEB,Y.GOTO,S.MORO and T.YAMAGUCHI , "Seismic Load Mitigation on LMFBR Reactor Building," *Atomic Energy Society of Japan*, 29,48-57 (1987)
[2] E,TADA, K.HADA and T.MARURO" Approach for Safety Assurance and Structural Integrity of ITER", *J. Plasma Fusion Res*, 78 ,1145-1156 (2002)
[3] S.KITAMURA,M.MORISHITA,S.YAZAWA and K.HIRATA," Ultimate behavior test of seismically isolated FBR plants with a large shaking (1) whole scheme " , *Atomic Energy Society of Japan Fall Meeting* (2008)
[4] S.KASAI,M.MAKOTO,K.MORIYA,T.IIKURA, "Development Status of HPABWRHPAPWR Interim Evaluation and Future Development Plans, " *Atomic Energy Society of Japan,*53,52-56 (2011)
[5] S.OKAMURA et al "Research and Development of Three-Dimensional Isolation System for SFR (Concept of Isolation System and Development Plan)", *Japan Society of Mechanical Engineers*, (2022)
[6] R.NAKANISHI et all," Fragility evaluation of base-isolated building : Part1: Seismic response analysis considering bumping against retaining wall", *Proceedings of the Architectural Institute of Japan*, B2, PP941-942(2007)
[7] T.NAKAZAWA et al, "Fundamental Study on Probabilistic Evaluation of the Ultimate State of Base Isolated Structures", *Transactions of AIJ. Journal of structural and construction engineering,* No.662, pp745-754
[8] A. SAREBANHA, G. MOSQUENDA, M. K. KIM, J. H. KIM," Effect of Moat Wall Impact on the Seismic Response of base Isolated Nuclear Power Plants", *16th World Conference on Earthquake*
[9] K.HIRATA,Y.OHTORI and T.SOMAKI, "Seismic Fragility Analysis for Base- Isolated Structure" *Transactions of AIJ. Journal of structural and construction engineering*, No.452, pp11-19
[10] Ark information system, seismic resistant and structure analysis series TDAPIII, https://www.ark-info sys.co.jp/jp/product/tdap/tdap3/
[11] R.KOMINE ,Y.OHTORI "Preliminary research on Risk Assessment of Seismic Isolation system considering ultimate characteristics of laminated rubber bearing" , *Japan Society of Mechanical Engineers (No20-11) Dynamics and Design Conference collection of lectures,* (2020)
[12] G.MIWATA et al "Experiments and Simulation Analysis of Collision to Retaining Wall with Real Scale Base-Isolated Building", unpublished,(2010)
[13] S.YABANA,K.KANAWAZA,S.NAGATA,KHIRATA,M.MOTOHASHI,S.KITAMURA," Ultimate Behavior of Base Isolated Structure Model Using E-defense Shaking Table" , N13,116 (2011)
[14] "A Study on the Analysis Time Step Required for Retaining-Wall Impacts in Base-Isolated Structures" , https://www.unions.co.jp/dqs/dynamic/techinfo/files/47.pdf (2018)
[15] Y.KIKUCHI," Seismic Safety Evaluation of Base-Isolated Structures", Ph.D. dissertation, Hokkaido University,1995
[16] Y.HAYASHI," Seismic Risk Evaluation of Existing RC Buildings Based on Seismic Performance Indices", "Social Safety Science",No.2, pp235-242,(2000)
[17] "Homepage of Mineo Takayama" https://www.4menshin.net/report/b_vol13/vol13_2.html, (2004)
[18] G.SHINDO," Fragility evaluation of base-isolated building : Part2 : Evaluation of fragility curve considering bumping against retaining wall", *Proceedings of the Architectural Institute of Japan*, B2, PP943-944(2007)
[19] H.TSUNEKAWA,M.FUZIMURA,Y.SATO,H.OKAMOTO," Probable Maximum Loss Based Seismic Performance Estimates of Reinforced Concrete Using Member-to-Member Dynamic Elasto-Plastic Analyses", *AIJ J. Technol Des* ,Vol.17, No.35, pp37-42,2011
[20] Y.KATAYAMA, "Trial design of box culverts using damage probability as an indicator2021" , unpublished ,(2022)
[21] Armin Masroor and Gilberto Mosqueda," Seismic Response of Base Isolated Buildings Considering Pounding to Moat Walls", *Technical Report MCEER-13-0003*,pp188-190,2013
[22] H.MIYANO et al "Standard of the Atomic Energy Society of Japan Criteria for Probabilistic Safety Assessment of Nuclear Power Plants due to Earthquakes",P346, Atomic Energy Society of Japan, Tokyo, 2007